Effects of Oligoelements Se, Zn, and Mn plus Lachesis Muta Venom in Experimental Scleroderma

Ernesto J. V. Crescenti, Vanina A. Medina, Lorena A. Sambuco, Graciela A. Cremaschi, Ana M. Genaro, Graciela P. Cricco, et al.

Biological Trace Element Research

ISSN 0163-4984

Biol Trace Elem Res
DOI 10.1007/s12011-013-9876-4

Springer

Biol Trace Elem Res
DOI 10.1007/s12011-013-9876-4

Effects of Oligoelements Se, Zn, and Mn plus Lachesis Muta Venom in Experimental Scleroderma

Ernesto J. V. Crescenti · Vanina A. Medina · Lorena A. Sambuco · Graciela A. Cremaschi · Ana M. Genaro · Graciela P. Cricco · Gabriela A. Martín · Eduardo Valli · Diego J. Martinel Lamas · Juan C. Perazzo · Elena S. Rivera · Rosa M. Bergoc

Received: 11 November 2013 / Accepted: 6 December 2013

Abstract Scleroderma, sclerosis of the skin, is a severe autoimmune disease refractant to all kind of treatments. To study the in vivo effects of a combination of three oligoelements selenium (Se), zinc (Zn), and manganese (Mn) plus Lachesis muta venom (O-LM) on the bleomycin (BLM)-induced scleroderma mouse experimental model. C3H mice were randomly divided into four groups: control (phosphate-buffered saline (PBS)), O-LM, BLM, and BLM+O-LM. All administrations were performed subcutaneously into the back of mice. BLM was injected 5 days per week for three consecutive weeks and O-LM was administered simultaneously with BLM from the beginning of the experiments and lasted for 3 weeks after the final BLM or PBS injection (for O-LM and BLM+O-LM groups), when animals were sacrificed and histopathological, immunohistochemical, thiobarbituric acid reactive species (TBARS) evaluation, and autoantibodies detection were determined. O-LM significantly reduced BLM-induced enhanced dermal thickness (605±47 vs. 956±59 μm, $P<0.01$), collagen deposition, and mast cells infiltration (43.1±1.0 vs. 102±14.1 mast cells, $P<0.05$). O-LM administration significantly blocked BLM-induced oxidative damage and the enhanced immunoreactive fibroblasts for α-smooth muscle actin while reduced BLM-induced autoantibodies that strongly react mainly with skin and spleen. O-LM significantly reduced BLM-induced scleroderma through the modulation of antioxidant and immunological pathways.

Keywords Scleroderma · Skin · Bleomycin · Oligoelements · Mouse

E. J. V. Crescenti · L. A. Sambuco
Institute of Immunooncology,
3200 Córdoba Av., 1187, Buenos Aires, Argentina

V. A. Medina (✉) · G. P. Cricco · G. A. Martín · D. J. Martinel Lamas · E. S. Rivera · R. M. Bergoc (✉)
Radioisotopes Laboratory, School of Pharmacy and Biochemistry, University of Buenos Aires,
Junín 956 1113, Buenos Aires, Argentina
e-mail: vmedina@ffyb.uba.ar
e-mail: rmbergoc@gmail.com

G. A. Cremaschi · A. M. Genaro · E. Valli
Neuroimmunomodulation and Molecular Oncology Division, Institute for Biomedical Research, Catholic University from Argentina (UCA), Buenos Aires, Argentina

V. A. Medina · G. A. Cremaschi · A. M. Genaro · G. A. Martín · E. Valli
National Research Council of Argentina (CONICET), Buenos Aires, Argentina

J. C. Perazzo
Pathophysiology, School of Pharmacy and Biochemistry, University of Buenos Aires, Buenos Aires, Argentina

Introduction

Systemic sclerosis (SSc) is a severe clinically heterogeneous disorder considered an autoimmune disease that displays a progressive accumulation of extracellular matrix components (ECM), which affects the connective tissue of the skin and internal organs such as gastrointestinal tract, lung, heart, and kidney with fibroblast activation [1, 2].

Cutaneous symptoms often associated with Reynaud's phenomenon and arthralgias of the fingers are usually early signs in the course of this disease. Patients with larger amount of cutaneous involvement are more likely to have problems in several organs. SSc can also affect any part of the gastrointestinal tract with severe consequences on nutritional status of patients. In this sense, the most common manifestation occurs in the esophagus [3]. Scleroderma, sclerosis of the skin, is the

Published online: 22 December 2013

typical symptom of SSc that affects the quality of patients' lives and is resistant to all kinds of treatments. As far as we know, the etiology, and the initial events of scleroderma remain unclear [4, 5], and no cure is clinically available [6, 7].

Experimental evidences sustain that the pathogenesis of scleroderma relies on immunological abnormalities and an increased oxidative stress [2, 5].

Over the last decades, different animal models have been investigated though none of them exhibits all aspects and chronic characteristics of human disease. One of the most characterized experimental models of scleroderma, which exhibits skin histological and biochemical changes similar to those of human scleroderma has been described by Yamamoto and co-workers. In this model, scleroderma is induced by means of a subcutaneous administration (back skin of mice) of bleomycin (BLM) [3, 8].

Bleomycin, a chemotherapeutic drug frequently used to treat various cancer types [9, 10], may produce side effects as scleroderma and lung fibrosis in patients. DNA damage and oxidative stress are involved in the molecular mechanisms of BLM-induced effects [3, 11]. It is also well known that oligoelements such as zinc (Zn), selenium (Se), and manganese (Mn) play a key role in both maintaining and reinforcing the immune and antioxidant performance [12-15]. Lachesis muta venom (LM) consists of a great variety of proteins, including phospholipase A2, which produces lysophosphatidylcholine with the ability to stimulate natural killer activity [16, 17].

We have previously demonstrated the protective effect of a novel combination of three oligoelements Se, Zn, and Mn plus LM (O-LM) against high doses of chemotherapy and radiotherapy in normal rodent tissues due to its antioxidant properties [18-20].

Aim

Based on presented evidence, the aim of this work was to study the in vivo effects of O-LM on the BLM-induced scleroderma mouse experimental model.

Material and Methods

Animals and Treatments

Six-week-old BALB/C female mice were purchased from the Division of Laboratory Animal Production, School of Veterinary Sciences, University of La Plata, Buenos Aires, Argentina and 6-week-old C3H female mice were purchased from the Laboratory Animal Production, National Atomic Commission, Argentina. All animals were maintained in health care facility at 22 °C and 50 to 60 % humidity on a 12 h light/dark cycle with food and water available ad libitum.

The O-LM was a combination of the oligoelements Zn, Se, and Mn (4 μg ml^{-1} each) (Merk, Argentina) plus LM (4 ng ml^{-1}) (kindly provided by Iquitos, Dep. Loreto or Cenepa, Mamayaque, Perú). BLM (Gador, Argentina) was dissolved in phosphate-buffered saline (PBS) at a concentration of 1 mg ml^{-1}.

C3H mice were randomly divided into four groups: control (PBS), O-LM, BLM and BLM+O-LM. All administrations were performed subcutaneously into the back of mice. Where indicated, BLM (0.1 ml) was injected 5 days per week for three consecutive weeks and O-LM was administered simultaneously with BLM from the beginning of the experiments and lasted for 3 weeks after the final BLM or PBS injection (for O-LM and BLM+O-LM groups).

Histopathological, immunohistochemical, thiobarbituric acid reactive species (TBARS) evaluation and autoantibodies detection were determined after the total experimental period of 6 weeks when the animals were sacrificed by cervical dislocation. Body weight was also monitored.

To evaluate the potential protective effect of O-LM against BLM cytotoxicity, an additional experiment was performed in BALB/C mice using a double dose of BLM (0.2 ml) during an extra week (4 week).

Animal procedures were in accordance with recommendations from the Guide for the Care and Use of Laboratory Animals of the National Research Council, USA, 1996, and protocols were approved by the Institutional Committee for the Care and Use of Laboratory Animals and also by the Ethical and Educational Committee of the Institute of Immunooncology.

Histopathological and Immunohistochemical Studies

The back skin area was removed and was cut in two parts, one of them for histopathological evaluation. Also, samples of esophagus, spleen, and lung were obtained. Tissue samples were fixed with 10 % neutral buffered formalin and were embedded in paraffin and cut into serial sections of 4 μm thick. The histopathological characteristics were examined on tissue sections after hematoxylin–eosin (HE) and Giemsa staining. Microscopic observation was performed on an Axiolab Karl Zeiss microscope (Göttingen, Germany). Histopathological skin slices were assessed and scored to provide a quantitative measurement by using ImageJ, NIH software.

For immunohistochemical studies, specimens were deparaffinized and were placed in citrate buffer (10 mM, pH 6.0) at boiling temperature for antigen retrieval as we have previously described [19]. Endogenous peroxidase activity was blocked with 3 % hydrogen peroxide in distillated water. After blocking, tissues were incubated with primary rabbit anti-alpha-smooth muscle actin (α-SMA, 1:50, Abcam Inc.,

Cambridge, MA, USA) or goat 8-hydroxydeoxyguanosine (8-OHdG, 1:200, Millipore, Temecula, CA, USA) antibodies overnight in a humidified chamber at 4ºC. Immunoreactivity was detected by using horseradish peroxidase-conjugated anti-rabbit, or anti-goat IgG, as appropriate, and developed by diaminobenzidine staining (Sigma Chemical Co., St. Louis, MO, USA). Images were taken using a Canon PowerShot G5 camera (Tokyo, Japan).

TBARS Evaluation

The TBARS assay is a well-established method for screening and monitoring lipid peroxidation. The method used in the present study, was previously described [21]. Briefly, the second part of the removed skin was homogenized in phosphate buffer pH 7.4 and was transferred to a tube containing trichloroacetic acid, HCl, and 2-thiobarbituric acid. The mixture was boiled for 30 min and then centrifuged at 3,000 rpm for 20 min at 4ºC. The absorbance in the resulting pink-stained TBARS supernatants was determined in a spectrophotometer (Genesys 10 UV, Thermo Scientific) at 535 nm. The acid did not produce color when tested without the addition of the sample. A molar extinction coefficient of $\varepsilon = 1.56 \times 10^5\ M^{-1}\ cm^{-1}$ was used for calculations.

Membrane Preparation

Tissue from the skin, lung, liver, and spleen were homogenized at 4 °C in six volumes of 5 mmol L^{-1} Tris-HCl, 1 mmol L^{-1} $MgCl_2$, 0.25 mol L^{-1} sucrose, pH 7.5 in an Ultraturrax. The homogenate was centrifuged for 10 min twice at 3,000 g, then at 10,000 g, and 40,000 g at 4 °C for 15 and 90 min, respectively. Microsomal pellets were finally resuspended in 50 mmol L^{-1} phosphate buffer, pH 7.4, supplemented with 0.1 mmol L^{-1} phenylmethylsulfonyl fluoride, 1 mmol L^{-1} EDTA, 5 mg ml^{-1} leupeptin, 1 mmol L^{-1} aprotinin, and 1 mmol L^{-1} pepstatin A. Skin membranes were obtained from ears of euthanized adult mice. Ears were rinsed with PBS, split into dorsal and ventral halves, and placed in PBS containing 0.03 % trypsin (Invitrogen, Carlsbad, CA, USA), 0.01 % DNase I (Promega, Madison, WI, USA), 100 U mL^{-1} of penicillin, 100 μg mL^{-1} of streptomycin, and 4 μg mL^{-1} of amphotericin B at 4 °C overnight. On the next day, the epidermal layer was separated from the dermal layer, and both layers were incubated in PBS with 0.03 % trypsin at 37 °C for 20 min. Following incubation, tissues were cut into smaller pieces and homogenized as indicated for the other tissues. All extracts were stored at −80ºC until use [22].

Autoantibody Detection

Serum samples were obtained from the caudal vein and stored at −80°C. Tissue extracts were suspended in 2× sample buffer (62.5 mmol L^{-1} Tris-HCl, pH 6.8, 2 % sodium dodecyl sulfate (SDS), 10 % glycerol, 5 % 2-mercaptoethanol, and 5 % bromophenol blue), and proteins were separated by polyacrylamide gel electrophoresis. Briefly, samples (1 mg mL^{-1} total protein) were separated by electrophoresis in SDS-containing (12.5 %) polyacrylamide gels and then transferred to polyvinylidene difluoride (PVDF) membranes (Millipore Corporation Bedford, MA, USA). The same amount of protein was prepared for each organ. Blotted membranes were treated with 1:100 diluted serum from BLM, BLM–O-LM, O-LM, or control mice. The membranes were then reacted with 1:1,000 diluted horseradish peroxidase-conjugated rabbit IgG fraction against mouse IgG (Sigma Chemical Co., St. Louis, MO, USA) as a secondary antibody. Detection used an enhanced chemiluminescence system (GE Healthcare Bio-Sciences, USA) [23].

Antinuclear antibodies were detected by indirect immunofluorescence methods using human Hep-2 cell line slides (Biorad, USA) as substrate. Murine sera (diluted 1:10) from each group were incubated on the slides for 30 min at room temperature, followed by detection with FITC-labeled rabbit anti-mouse IgG (1:50, Sigma Aldrich, USA) according to the manufacturer's instructions.

Statistical Analysis

Data were analyzed using the GraphPad Prism 5.0 (Graph Pad Software Inc., CA, USA). *P* values less than 0.05 were considered as statistically significant.

Results

Effect of O-LM on BLM-induced Scleroderma

Histological studies in daily BLM-injected C3H mice for 3 weeks demonstrated marked dermal sclerosis characterized by increased dermal and vascular walls thickness and homogeneous collagen bundles that cross the subcutaneous adipose tissue (Fig. 1A, B).

In addition, an increase in α-SMA reactive fibroblasts was observed in BLM-injected group compared with that in control or O-LM groups (Fig. 1C, D). On the contrary, O-LM treatment simultaneously administered with BLM significantly decreased the dermal thickness while completely prevented the collagen bundles spreading (Fig. 1A, B) and also reduced the number of α-SMA positive cells (1.4±0.1 vs. 5.8±0.2 in BLM group, $P<0.05$) (Fig. 1C, D).

Inflammatory infiltrates were observed in the deeper dermis layer in the BLM-injected animals. Giemsa staining showed a 2.5-fold increase in the number of mast cells around sclerotic lesions in BLM group (Fig. 2A, B). Notably, O-LM

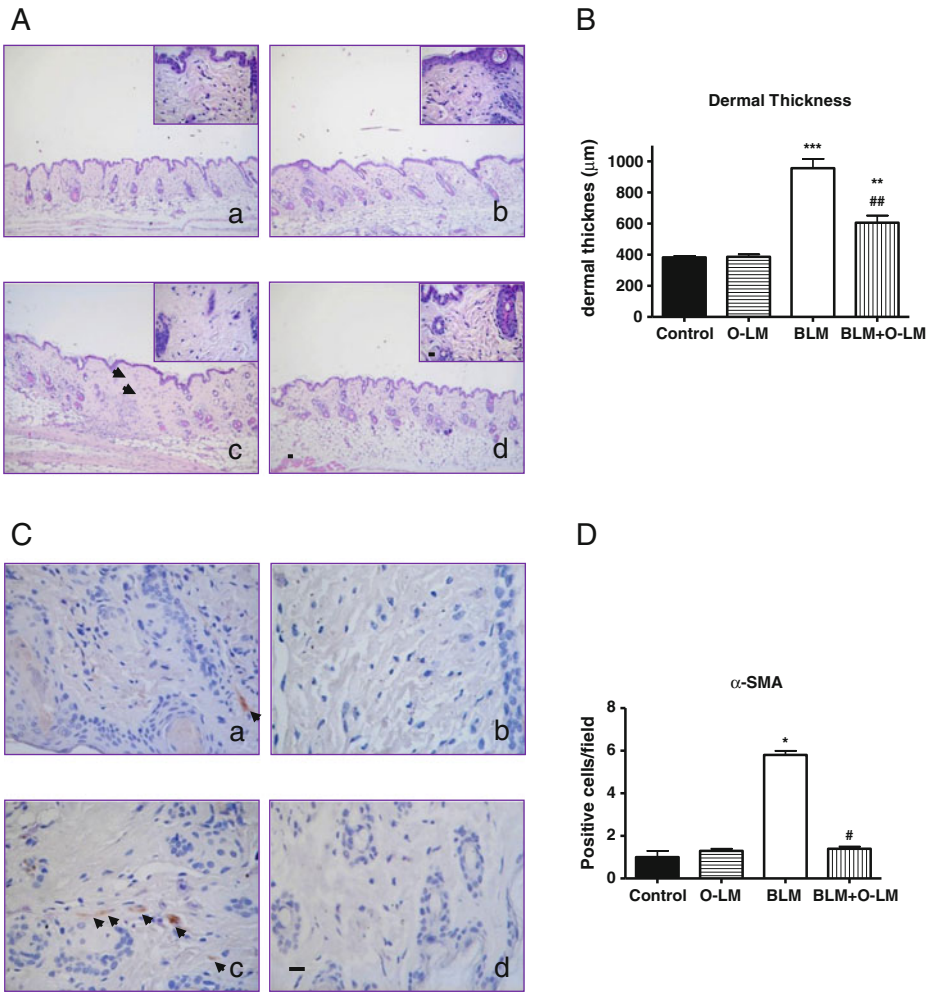

Fig. 1 Histopathological and morphometrical evaluation in scleroderma developed in C3H mice. **A** Representative histological changes of skin 3 weeks after cessation of BLM injection (*a*, *b*, *c*, *d*). (*c*) Collagen bundles with homogeneous deposition are observed (*arrows*) in skin of BLM-injected mice (0.1 ml per day for 3 weeks) while normal features are displayed in (*a*) control (PBS-treated), (*b*) O-LM treated (0.1 ml per day simultaneous administration until the end of the experiment), (*d*) BLM-injected and O-LM-treated mice. HE staining. Original magnification 630× and 100×, *scale bar*=20 μm. **B** *Dermal thickness.* Significant differences were observed in dermal thickness between BLM-injected and BLM-injected and O-LM-treated animals. Data represent the mean± SEM (n=10 each group). **P<0.01, ***P<0.001 vs. control; ##P<0.01 vs. BLM group (one-way ANOVA followed by Tukey post test). **C**, **D** *Immunohistochemical analysis of* α*-SMA.* **C** Representative pictures of each group are shown. (*a*) Control group (PBS-treated), (*b*) O-LM-treated mice (0.1 ml per day for 3 weeks) and (*d*) BLM-injected C3H mice plus O-LM-treatment displayed normal epidermal and dermal features. (*c*) BLM-injected mice (0.1 ml per day for 3 weeks) showed increased positive fibroblastic cells for α-SMA. Original magnification 630×, *scale bar*=20 μm. **D** Positive fibroblastic cells for α-SMA in 10 random fields are depicted. Data represent the mean±SEM (n=5 each group). *P<0.05 vs. control; #P<0.05 vs. BLM group (nonparametric Kruskal–Wallis test, Dunns post test)

completely blocked the mast cells dermal infiltration (43.1± 1.0 vs. 102±14.1 in BLM group, P<0.05) (Fig. 2A, B).

Role of O-LM in BLM-induced Oxidative Stress

8-OHdG formation was evaluated by immunohistochemistry as a marker of oxidative damage. Weak 8-OHdG immunoreactivity in few epidermal and dermal cells was observed in control and O-LM-injected animals. BLM-injected C3H mice exhibited a remarkable increase in the number of 8-OHdG positive cells in dermis and also in epidermis (Fig. 3A). Conversely, O-LM administration notably decreased the immunoreactivity for 8-OHdG (Fig. 3A). In addition, O-LM administration suppressed BLM-induced enhanced TBARS levels, a marker of lipid peroxidation (Fig. 3B).

Effect of O-LM in Other Parameters Modified by BLM

In order to determine whether O-LM treatment could modulate BLM-induced autoantibodies, sera from BLM-injected C3H mice were analyzed by western blot. Several bands corresponding to autoantibodies against normal tissues

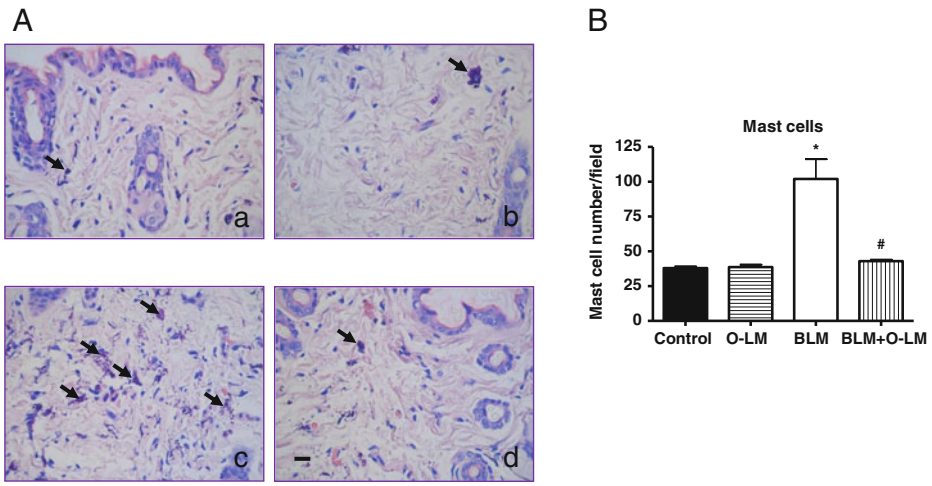

Fig. 2 Changes on mast cells number. **A** Representative pictures of each group. (*a*) Control (PBS-treated), (*b*) O-LM treated (0.1 ml per day simultaneous administration until the end of the experiment), (*c*) BLM-injected (0.1 ml per day for 3 weeks), and (*d*) O-LM-treated and BLM-injected C3H mice. Giemsa staining. *Arrows* indicate mast cells. Original magnification 630×, *scale bar*=20 μm. **B** Mast cell count. The number of mast cells in 10 random 100× fields is depicted. Data represent the mean± SEM (n=10 each group). *P<0.05 vs. control; #P<0.05 vs. BLM group (nonparametric Kruskal–Wallis test, Dunns post test)

including murine skin, lung, and spleen were detected using sera of BLM-injected mice. These bands were considerable decreased in O-LM-administered mice (Fig. 4A). It is important to note that autoantibodies were not detected using sera of control or O-LM-treated mice (data not shown).

In addition, nuclear staining was observed on Hep-2 cells using sera of BLM-injected mice, whereas a reduced staining was observed using sera of O-LM treated mice (Fig. 4B).

Histopathological analysis of all organs demonstrated that the esophagus was the main internal organ that exhibited significant alterations. The main histopathological feature in the esophagus of BLM-injected C3H mice was the significant enlargement of esophageal wall due to thickening of the muscle layer, compared with the control and O-LM-treated mice. The muscle layers showed a very significant increase in collagen deposited between muscle fibers and the absence of inflammatory cells neighboring muscle cells (Fig. 5A). Interestingly, O-LM treatment reduced the BLM-induced enhanced esophagus enlargement and also decreased the collagen deposits (Fig. 5A).

Additionally, a significant decrease in body weight was observed in C3H mice along the 3 weeks of BLM

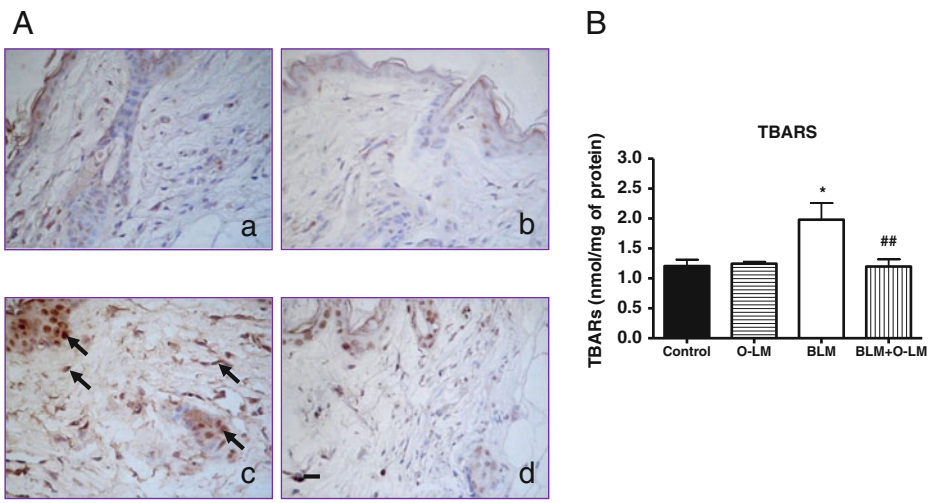

Fig. 3 Evaluation of oxidative stress. **A** Immunohistochemical analysis of 8-OHdG. Representative pictures of each group are shown. (*a*) Control (PBS-treated), displayed weak 8-OHdG immunoreactivity in both, epidermal and dermal cells. (*b*) O-LM-treated (0.1 ml per day simultaneous administration until the end of the experiment) showed similar features as in control group. (*c*) BLM-injected (0.1 ml per day for 3 weeks) showed marked immunoreactivity in epidermal and dermal cells (*arrows*) while (*d*) BLM-injected and O-LM-treated C3H mice exhibited normal dermal features and weak epidermal positive cells. Original magnification 630×, *scale bar*=20 μm. **B** Determination of TBARS. Data represent the mean± SEM (n=6 each group). *P<0.05 vs. control; ##P<0.01 vs. BLM group (one-way ANOVA followed by Tukey post test)

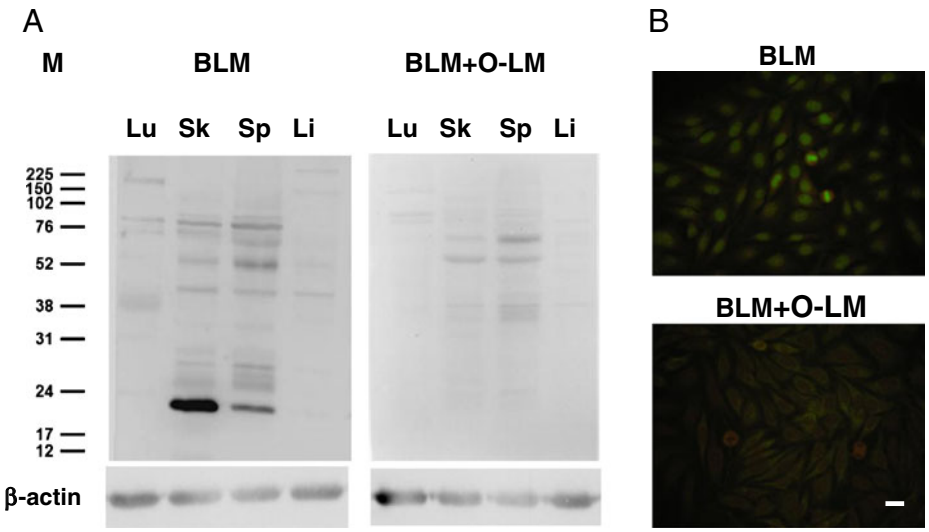

Fig. 4 Detection of serum antibodies. **A** Autoantibodies binding to murine tissue proteins. Tissue proteins (30 μg per lane) from normal C3H lung (Lu), skin (Sk), spleen (Sp), and liver (Li) extracts were run in SDS-PAGE and transferred to PVDF membranes. Serum samples from BLM-injected mice (0.1 ml per day for 3 weeks) and BLM-injected and O-LM-treated mice were used to reveal the presence of autoantibodies. *M* molecular weight marker. β-actin was used as load control. Results shown are representative from three different experiments. **B** Detection of antinuclear antibodies by immunofluorescence method using Hep-2 targets. Original magnification 400×, *scale bar*=20 μm

administration, effect that was completely prevented by O-LM administration (Fig. 5B).

Effect of O-LM on BLM-Induced Cytotoxicity

We additionally investigated whether O-LM could prevent BLM-induced cytotoxicity in BALB/C, a more chemoresistant strain of mice [3, 24]. BML administration was performed at a higher concentration (0.2 ml per day) during an additional week (4 weeks in total) in BALB/C mice. Results show that 60 % of mice died 2 days after cessation of BLM injection (at a higher concentration) while all animals receiving O-LM survived (Fig. 6A).

Histopathological studies demonstrated that the main reason of death in BLM-injected animals was lung injury, which includes thickening in the septal wall, congestion, and secondary inflammatory chronic reaction with collagen deposits (Fig. 6B).

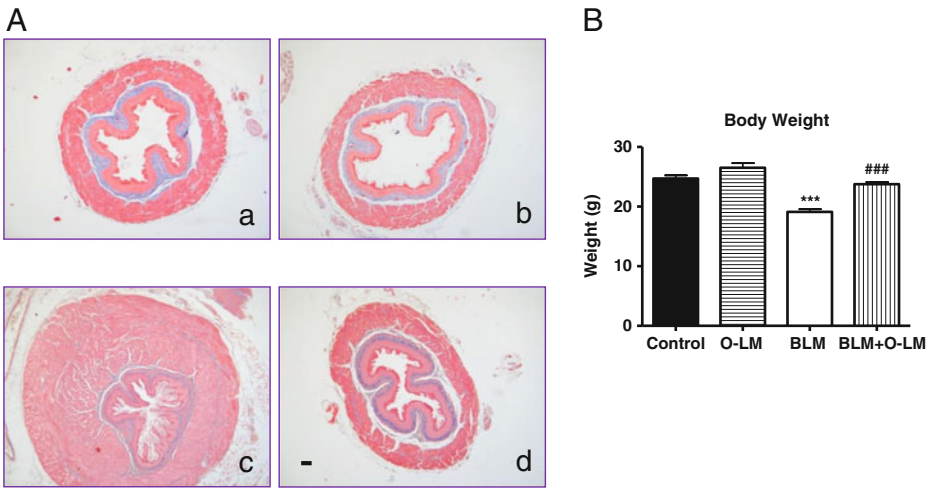

Fig. 5 Esophageal histopathology and body weight. **A** Esophageal changes. (*a*) Control (PBS-treated), (*b*) O-LM-treated (0.1 ml per day), and (*d*) O-LM-treated and BLM-injected C3H mice showed normal features. (*c*) BLM-injected animals (0.1 ml per day for 3 weeks) exhibited a diffuse sclerosis in the submucosal and muscular layers with increased wall thickness. Masson's trichrome technique. Original magnification 50×, *scale bar*=50 μm. **B** Body weight of C3H mice. Data represent the mean±SEM (n=10 each group). ***P<0.001 vs. control; ###P<0.001 vs. BLM group (one-way ANOVA followed by Tukey post test)

A

Group	Survival Fraction
Control	10/10
O-LM	10/10
BLM	4/10**
BLM+O-LM	10/10

B

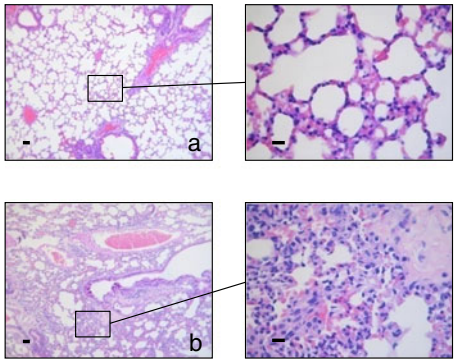

Fig. 6 Cytotoxicity studies in BALB/C mice. **A** Kaplan–Meier analysis. Data represent the fraction of animals, which survived after 4 weeks of BLM administration (0.2 ml per day). (**$P<0.0043$, Log rank and Gehan–Breslow–wilcoxon tests) ($n=10$ each group). **B** Lung histopathology. (*b*) BLM-injected mice (0.2 ml per day for 4 weeks) showed thickening in the septal wall, congestion with focal hemorrhage. (*a*) BLM-injected and O-LM-treated mice exhibited normal features. HE. Original magnification 100× and 630×, *scale bar*=20 μm

Discussion

Scleroderma is a severe, fibrotic condition characterized by immunological abnormalities, microvascular damage, fibroblast activation, and increased accumulation of extracellular matrix proteins in the skin. Furthermore, recent evidences support the role of oxidative stress in the pathogenesis of this autoimmune disease [2, 5]. Novel treatments for scleroderma are therefore of utmost importance. In the present study, we demonstrated the beneficial potential of O-LM on BLM-induced scleroderma in a well-known experimental mouse model. A marked dermal sclerosis and a rise in mast cell number were observed in C3H mice 3 weeks after cessation of BLM administration as it was previously described [8]. O-LM administration significantly reduced BLM-induced enhanced dermal thickness, collagen deposition, and mast cells infiltration. Mast cells have a direct and potentiating function in skin remodeling and fibrosis since increased numbers of mast cells and myofibroblasts were frequently found together in wound repair and scleroderma skin [25, 26]. Therefore, the lower number of mast cells observed in the lesional skin of the O-LM+BLM group might be involved in the lessened sclerotic response.

Although the etiology of scleroderma has not yet been fully elucidated, a growing body of evidence suggests that ECM overproduction by activated fibroblasts results from intricate interactions among endothelial cells, lymphocytes, macrophages, and fibroblasts [27]. Activated fibroblasts or myofibroblast are characterized by the expression of α-SMA and the increased production of ECM, two relevant features of connective tissue remodeling [3]. Our current study shows that O-LM administration reduced BLM-induced enhanced immunoreactive fibroblasts for α-SMA in lesional skin, in accordance with other reports [28].

Increased free radical production is also supposed to be involved in the pathogenesis of scleroderma as an important initiator of tissue damage [5]. BLM is known to generate reactive oxygen species (ROS), which are involved in BLM-induced scleroderma, indicating that antioxidant therapy may lead to antifibrotic effects. Yamamoto *et. al* demonstrated that administration of superoxide dismutase inhibits BLM-induced dermal sclerosis in the same experimental model [4]. ROS at a high concentration can damage DNA, lipids, and proteins [5]. Formation of 8-OHdG is a well-known DNA oxidative marker while TBARS evaluation is used as an indicator of lipid peroxidation [5]. Higher 8-OHdG urinary levels were found in scleroderma patients [27]. In the present work, we demonstrate that O-LM administration significantly blocked BLM-induced oxidative damage, reducing 8-OHdG formation and lipid peroxidation levels. In agreement with these results, it was reported that plasma lipid peroxidation was markedly increased while Se levels were reduced in SSc patients [29].

Autoantibodies are also related to the pathogenesis of human scleroderma, and they are increased in BLM-induced scleroderma experimental model [8, 30]. Therefore, autoantibodies were further investigated in sera from all groups. Our experiments demonstrate that BLM increased sera autoantibodies, which mainly reacted with skin and spleen. This effect was almost blocked by O-LM administration. In addition, the presence of antinuclear antibodies in sera of BLM group were confirmed employing Hep-2 targets, while were not observed using sera of O-LM-treated mice, indicating that modulation of immune system is involved in the mechanisms of action of this novel formulation.

Impairment of gastrointestinal tract with esophageal fibrosis is a common manifestation of SSc [30]. In our study, histopathological analysis of all organs demonstrated that the esophagus was the main organ that exhibited significant alterations. BLM produced enlargement of esophageal wall with thickened muscle layer and increased collagen deposits, leading to lumen reduction.

Furthermore, body weight was significantly decreased, effect that could be associated with the cytotoxicity of BLM as it was previously described [30]. Interestingly, O-LM administration completely prevented BLM-induced esophageal and body weight alterations suggesting that O-LM is able to reduced BLM-induced cytotoxic effects.

Previous reports show that C3H mice are more susceptible to BLM-induced damage than BALB/C mice [3, 24]; therefore, we additionally investigated the O-LM efficacy on preventing BLM-induced toxicity, employing more chemoresistant strain, BALB/C. Surprisingly, a significant increased survival in BALB/C mice that received BLM and O-LM was observed, suggesting that O-LM efficiently reduced BLM-induced toxicity. Histopathological studies indicate that lung injury was likely the main reason of death. In agreement with these results, lung fibrosis is a well-known side effect induced in patients treated with BLM [3].

Furthermore, additional studies demonstrate that after onset of BLM-induced scleroderma, which closely reflects a clinical situation of existing dermal sclerosis, O-LM administration (initiated after cessation of BLM injection) significantly reversed some parameters investigated including dermal thickness (687.9±76.6 μm vs. 1135.2±102.2 μm in BLM group, $P<0.001$).

In conclusion, presented results clearly show that the combination of these three oligoelements (Zn, Se, and Mn) plus LM administration significantly reduced BLM-induced scleroderma through the modulation of antioxidant and immunological pathways.

Acknowledgments We dedicate this work to the memory of our friend, colleague, and excellent pathologist Maximo Croci, MD. We thank Alejandro Paredes for technical assistance. V. Medina, G. Martín, A. Genaro, G. Cremaschi and R. Bergoc are members of the National Research Council (CONICET).

Conflict of interest Authors declared no conflict of interest.

References

1. Varga J, Abraham D (2007) Systemic sclerosis: a prototypic multisystem fibrotic disorder. J Clin Invest 117:557–567
2. Yamamoto T (2011) Autoimmune mechanism of scleroderma and role of oxidative stress. SelfNonself 2:4–10
3. Yamamoto T, Nishioka K (2005) Cellular and molecular mechanisms of bleomycin-induced murine scleroderma: current update and future perspective. Exp Dermatol 14:81–95
4. Yamamoto T, Takagawa S, Katayama I, Mizushima Y, Nishioka K (1999) Effect of superoxide dismutase on bleomycin-induced dermal sclerosis: implications for the treatment of systemic sclerosis. J Investig Dermatol 113:843–847
5. Gabrielli A, Svegliati S, Moroncini G, Amico D (2012) New insights into the role of oxidative stress in scleroderma fibrosis. Open Rheumatol J 6:87–95
6. Nitsche A (2012) Raynaud digital ulcers and calcinosis in scleroderma. Reumatol Clin 8:270–277
7. Zulian F, Vallongo C, Patrizi A, Belloni-Fortina A, Cutrone M, Alessio M, Martino S, Gerloni V, Vittadello F, Martini G (2012) A long-term follow-up study of methotrexate in juvenile localized scleroderma (morphea). J Am Acad Dermatol 67:1151–1156
8. Yamamoto T, Takagawa S, Katayama I, Yamazaki K, Hamazaki Y, Shinkai H, Nishioka K (1999) Animal model of sclerotic skin. I: Local injections of bleomycin induce sclerotic skin mimicking scleroderma. J Investig Dermatol 112:456–462
9. Povirk LF, Austin H (1991) Genotoxicity of bleomycin. Mutat Res 257:127–143
10. Tokuhashi Y, Kikkawa F, Tamakoshi K, Suganuma N, Kuzuya K, Arii Y, Kawai M, Hattori S, Kobayashi I, Furuhashi Y, Nakashima N, Tomoda Y (1997) A randomized trial of cisplatin, vinblastine, and bleomycin versus cyclophosphamide, aclacinomycin, and cisplatin in epithelial ovarian cancer. Oncology 54:281–286
11. Abraham AT, Lin JJ, Newton DL, Rybak S, Hecht SM (2003) RNA cleavage and inhibition of protein synthesis by bleomycin. Chem Biol 10:45–52
12. Wintergerst EV, Maggini E, Horning DH (2007) Contribution of selected vitamins and trace elements to immune function. Ann Nutr Metab 51:301–323
13. Saper RB, Rash R (2009) Zinc: an essential micronutrient. Am Fam Physician 79:768–772
14. Kehl-Fie TE, Skaar EP (2010) Nutritional immunity beyond iron: a role for manganese and zinc. Curr Opin Chem Biol 14:218–224
15. Rayman MP (2012) Selenium and human health. Lancet 379:1256–1268
16. Fuly AL, Machado AL, Castro P, Abrahão A, Redner P, Lopes UG, Guimarães JA, Koatz VL (2007) Lysophosphatidylcholine produced by the phospholipase A2 isolated from Lachesis muta snake venom modulates natural killer activity as a protein kinase C effector. Toxicon 50:400–410
17. Sanz L, Escolano J, Ferretti M, Biscoglio MJ, Rivera E, Crescenti EJ, Angulo Y, Lomonte B, Gutiérrez JM, Calvete JJ (2007) Snake venomics of the South and Central American Bushmasters. Comparison of the toxin composition of Lachesis muta gathered from proteomic versus transcriptomic analysis. J Proteome 71:46–60
18. Crescenti E, Croci M, Rivera E, Bergoc R (2003) Enhanced tolerante to high cytostatic doses by means of oligoelements Mn, Se and Zn plus Lachesis muta venom. J Trace Elem Exp Med 16:39–53
19. Crescenti E, Croci M, Medina V, Sambuco L, Bergoc R, Rivera E (2009) Radioprotective potential of a novel therapeutic formulation of oligoelements Se, Zn, Mn plus Lachesis muta venom. J Radiat Res 50:537–544
20. Crescenti EJ, Medina VA, Croci M, Sambuco LA, Prestifilippo JP, Elverdin JC, Bergoc RM, Rivera ES (2011) Radioprotection of sensitive rat tissues by oligoelements Se, Zn, Mn plus Lachesis muta venom. J Radiat Res 52:557–567
21. Shvedova AA, Kisin ER, Murray A, Kommineni C, Vallyathan V, Castranova V (2004) Pro/antioxidant status in murine skin following topical exposure to cumene hydroperoxide throughout the ontogeny of skin cancer. Biochemistry (Mosc) 69:23–31
22. Cremaschi G, Zwirner NW, Gorelik G, Malchiodi EL, Chiaramonte MG, Fossati CA, Sterin-Borda L (1995) Modulation of cardiac physiology by an anti-Trypanosoma cruzi monoclonal antibody. FASEB J 9:1482–1488
23. Barreiro Arcos ML, Sterle HA, Paulazo MA, Valli E, Klecha AJ, Isse B, Pellizas CG, Farias RN, Cremaschi GA (2011) Cooperative nongenomic and genomic actions on thyroid hormone mediated-modulation of T cell proliferation involve up-regulation of thyroid hormone receptor and inducible nitric oxide synthase expression. J Cell Physiol 226:3208–3218

24. Yamamoto T, Kudoka M, Nishioka K (2000) Animal model of sclerotic skin. III: histopathological comparison of bleomycin-induced scleroderma in various mice strains. Arch Dermatol Res 292:535–541
25. Gailit J, Marchese MJ, Kew RR, Gruber BL (2001) The differentiation and function of myofibroblasts is regulated by mast cell mediators. J Investig Dermatol 117:1113–1119
26. Garbuzenko E, Nagler A, Pickholtz D, Gillery P, Reich R, Maquart FX, Levi-Schaffer F (2002) Human mast cells stimulate fibroblast proliferation, collagen synthesis and lattice contraction: a direct role for mast cells in skin fibrosis. Clin Exp Allergy 32: 237–346
27. Avouac J, Borderie D, Ekindjian OG, Kahan A, Allanore Y (2010) High DNA oxidative damage in systemic sclerosis. J Rheumatol 28: 2540–2547
28. Yamamoto T, Nishioka K (2002) Animal model of sclerotic skin. V: increased expression of alpha-smooth muscle actin in fibroblastic cells in bleomycin-induced scleroderma. Clin Immunol 102:77–83
29. Tikly M, Channa K, Theodorou P, Gulumian M (2006) Lipid peroxidation and trace elements in systemic sclerosis. Clin Rheumatol 25:320–324
30. Ishikawa H, Takeda K, Okamoto A, Matsuo S, Isobe K (2009) Induction of autoimmunity in a bleomycin-induced murine model of experimental systemic sclerosis: an important role for CD4+ T cells. J Investig Dermatol 129:1688–1695